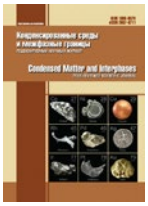

ISSN 1606-867X (Print)
ISSN 2687-0711 (Online)
Condensed Matter and Interphases
Kondensirovannye Sredy i Mezhfaznye Granitsy
https://journals.vsu.ru/kcmf/

Original articles

Research article
https://doi.org/10.17308/kcmf.2023.25/11484

A study of gallium oxide by using the piezoelectric composite oscillator technique at a frequency of 100 kHz

V. V. Kaminskii✉, D. A. Kalganov, D. I. Panov, V. A. Spiridonov, A. Yu. Ivanov, M. V. Rozaeva, D. A. Bauman, A. E. Romanov

ITMO University,
49 Kronverksky pr., St. Petersburg 197101, Russian Federation

Abstract

The article presents the results of the study of the mechanical properties and defect structure of gallium oxide (Ga_2O_3) by using the piezoelectric composite oscillator technique. Bulk samples of the Ga_2O_3 beta phase in the form of single crystals and their intergrowths were obtained by growth from a melt with a shaper (Stepanov technique). The research involved studying the dependences of the longitudinal elastic modulus and the damping of elastic vibrations at a frequency of 100 kHz on the strain amplitude. Changes in the elastic and microplastic properties of the samples at different temperatures were attributed to possible relaxation phenomena in the structure of the material.

Studying the defect structure in samples of pure and doped Ga_2O_3 is necessary to improve the technology for the production of large single crystals. The fundamental questions in this area are the influence of defects on the anisotropy of electrical conductivity, band structure, and other functional properties of the resulting semiconductor material. The purpose of this article is to establish the features of sample preparation, research, and interpretation of the results obtained by the piezoelectric composite oscillator technique for gallium oxide samples.

In the studied samples, the first longitudinal vibration mode was excited, which corresponded to a length of about 27 mm and a small cross-section of the sample. The temperature dependences in the region of low and high strain amplitudes were determined separately. The crystalline quality of the prepared samples was assessed by X-ray diffraction with the analysis of the rocking curve.

The value of Young's modulus obtained along the growth axis (crystalline orientation <010>) in Ga_2O_3 crystals E≈260 GPa is in line with the results of previous studies. Relaxation peaks corresponding to various dislocation interactions were found on the temperature dependences of internal friction at a temperature of 280 K.

Keywords: Gallium oxide, Single crystal, Defect structure, Real structure, Semiconductor, Piezoelectric composite oscillator technique

Funding: This work was supported by the grant of Russian Science Foundation No. 19-19-00617.

For citation: Kaminskii V. V., Kalganov D. A., Panov D. I., Spiridonov V. A., Ivanov A. I., Rozaeva M. V., Bauman D. A., Romanov A. E. A study of gallium oxide by using the piezoelectric composite oscillator technique at a frequency of 100 kHz. *Condensed Matter and Interphases*. 20223;25(4): 548–556. https://doi.org/10.17308/kcmf.2023.25/11484

Для цитирования: Каминский В. В., Калганов Д. А., Панов Д. Ю., Спиридонов В. А., Иванов А. Ю., Розаева М. В., Бауман Д. А., Романов А. Е. Исследование оксида галлия методом составного пьезоэлектрического осциллятора на частоте 100 кГц. *Конденсированные среды и межфазные границы*. 2023;25(4): 548–556. https://doi.org/10.17308/kcmf.2023.25/11484

✉ Vladimir V. Kaminskii, e-mail: vvkaminskii@itmo.ru

1. Introduction

The search for new techniques for the manufacture and study of large-sized single crystals of β-Ga_2O_3 is associated with the possibility to use them to create substrates and functional parts for semiconductor devices [1]. Due to the unique properties of various forms of gallium oxide, it can be used to miniaturize existing power electronics components and to develop new ones [2, 3]. In this case, β-Ga_2O_3 substrates will allow using the advantages of homoepitaxy, simplifying the production technology, and ensuring the durability of the finished devices [4]. Applications of Ga_2O_3 for the creation of ultraviolet [5, 6] and X-ray detectors [7], gas sensors [8, 9], and other devices [10] have also been described. Currently, the largest linear dimensions of produced single crystals of β-Ga_2O_3 are up to 11 cm [11]. Intrinsic defects (oxygen vacancies [12]) and unintentional alloying which occur in the process of growth, as a rule, have a negative impact on their functional properties [13, 14]. However, the control of the density and distribution of defects of various types can allow the thermal conductivity, electrical conductivity, band structure, and many other properties of crystals to be purposefully changed [15, 16].

The defect-impurity structure of semiconductors has been widely studied by methods based on their optical and electronic radiofrequency properties [13, 17]. The band structure of Ga_2O_3 and its other properties which are important for solving applied problems have been studied analytically [18], numerically, and comprehensively [19]. However, one of the most universal techniques of structure analysis is based on the interaction of defects with the field of elastic waves [20, 21]. The piezoelectric composite oscillator (PCO) technique has been widely used to excite elastic vibrations [22]. Depending on the temperature, crystal orientation, and vibration frequency and amplitude, such interactions will have different values of energy loss due to internal friction [21, 23]. The maximum sensitivity of the PCO technique to the interaction of dislocations with point defects of various kinds is achieved at strain amplitudes from 10^{-7} to 10^{-4} in the frequency range of $10^3 \div 10^6$ Hz [24, 25]. The amplitude-independent part of the damping of elastic vibrations makes it possible to construct so-called indicative surfaces of the internal friction background [23] and to determine the orientation and activity of the dislocation slip systems. The damping of high-amplitude vibrations characterizes various processes of dislocation reproduction and motion in the elastic fields of other defects [26].

Despite the large amount of data on the structural properties of β-Ga_2O_3 [27], scientists continue to research the activation of various dislocation slip systems [28, 29]. The mechanical properties of bulk crystals of β-Ga_2O_3 necessary for the effective manufacture of wafer substrates have also been poorly studied. The study of these properties appears to be challenging due to the strict requirements to the preparation of samples of the specified shape and size and due to the need for additional research by other techniques. In this regard, so far, studies of the mechanical properties of Ga_2O_3 have only been carried out by those techniques that could be adapted for measurements on thin films and small-sized crystals.

The purpose of this work is to study bulk Ga_2O_3 crystals by the piezoelectric composite oscillator technique at a frequency of 100 kHz and to obtain data on the elastic and plastic features of the mechanical characteristics of Ga_2O_3.

2. Experimental

Bulk crystals of β-Ga_2O_3 were produced by the liquid-phase growth technique from a melt with a shaper (Stepanov technique) [11, 12] (Fig. 1a).

In this paper, the piezoelectric composite oscillator (PCO) technique with a measurement frequency of about 100 kHz was used as the main method for studying mechanical properties [25, 26]. The experiments were carried out at strain amplitudes from 10^{-7} to 10^{-4} in a wide temperature range from 120 to 320 K.

A piezoelectric composite oscillator was two soldered quartz single crystals. The studied material was attached to the oscillator with

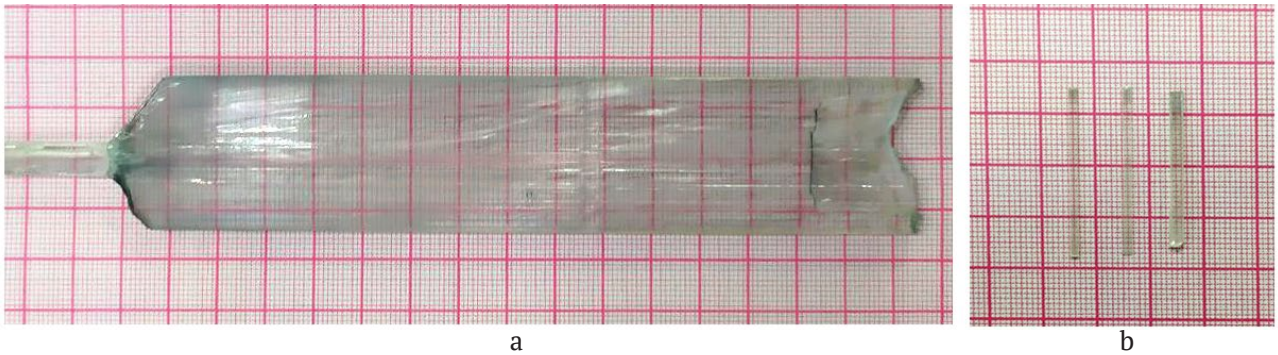

a b

Fig. 1. The appearance of the β-Ga_2O_3 bulk samples obtained by Stepanov edge-defined film-fed growth method (a) and samples prepared for investigation by composite oscillator technique (b)

various adhesive substances. When an alternating voltage was applied to the electrodes of one of the crystals, it started to oscillate and transmit elastic vibrations to the sample. The value of the damping coefficient was obtained from the ratio of the signal on the electrodes of the second measuring crystal to the first one. The oscillation frequencies of the entire system were also measured. The values of internal friction and elastic moduli were found by the measured values with due account of the characteristics of the quartz oscillator and the coupling coefficient. In this research, measurements were taken at a resonance frequency of about 100 kHz for the first longitudinal oscillation mode. In this case, the change in frequency corresponded to the value of the Young's modulus. The Young's modulus and internal friction determined by this technique provided cumulative information about the dynamic properties of the microstructure and their changes under the influence of deformations in the studied material:

$$m_{osc}\delta_{osc} = m_{qu}\delta_{qu} + m_{sam}\delta_{sam},$$
$$m_{osc}f_{osc} = m_{qu}f_{qu} + m_{sam}f_{sam},$$

where m_{osc} is the mass of the entire oscillator; m_{qu} is the mass of quartz; m_{sam} is the mass of the sample; δ_{osc} is the damping of vibrations on the entire oscillator; δ_{qu} is the damping the vibrations on quartz; δ_{sam} is the damping of vibrations on the sample; f_{osc} is the frequency of vibrations on the entire oscillator; f_{qu} is the frequency of vibrations on quartz; and f_{sam} is the frequency of vibrations on the sample.

The Young's modulus for the sample material is defined as:

$$E = 4\rho l^2 f_{sam}^2,$$

ρ is the density of the studied material; and l is the length of the sample.

The relative change in elastic properties associated with the heating of the sample and its reversible dislocational deformation is characterized by the Young's modulus defect. In the case of longitudinal oscillations, this value is determined from the ratio:

$$\Delta E = \frac{(E_i - E(\varepsilon))}{E_i},$$

where E_i is the elastic modulus at the amplitude-independent stage, $E(\varepsilon)$ is the elastic modulus at the amplitude-dependent stage, and ε is the strain amplitude of the sample.

For PCO measurements, a diamond-coated circular saw was used to prepare samples in the form of parallelepipeds with dimensions of about 27×2×1 mm^3. The long side of the samples coincided with the growth axis <010> and the propagation direction of elastic vibrations from the piezoelectric oscillator to the sample. To ensure reliable results, measurements were taken on three samples of the same type (Fig. 1b).

The density of the samples was determined by hydrodensitometry using GH-252 accuracy class III balances (A&D Company) and a V7-78/1 temperature meter (AKIP). For the studied material, the average density value was ρ = 5915±12 kg/m^3.

In this experiment, in addition to the PCO technique, an X-ray diffraction analysis (a DRON-8 diffractometer, CuK_α-radiation, slit configuration, BSV-29 tube, NaI-Tl detector) was used to assess the crystalline perfection of the studied samples. The crystals prepared

for the PCO were studied in continuous and discrete modes in a wide range of angles. Rocking curves for reflection maxima (12 0 0) were also studied. Since the maximum deforming stress during the first longitudinal mode is localized in the center of the sample, we studied this area. The size of the X-ray beam on the surface was approximately equal to the width of the sample of ~ 2 mm.

2. Results and discussion

The obtained diffraction data are shown in Fig. 2. The overall diffraction pattern (Fig. 2A) has clear plane diffraction peaks (1 0 0) of different diffraction orders. The profile and diffraction angles correspond to the PDF 01-087-1901 data. The sample was examined and positioned by reflection (12 0 0). Fig. 2b shows the reflection diffractograms in a discrete mode to determine $2\Theta K_{\alpha 1}$ = 102.24°. The rocking curve for the reflection maxima (12 0 0) was obtained with a narrow slit configuration in a discrete mode at two step values (Fig. 2c). The rocking curve profile has an asymmetric shape with a "tail" at smaller ω, the full width at half maximum intensity is approximately 0.011°.

The amplitude dependences of internal friction and Young's modulus were obtained by the PCO technique at room temperature (Fig. 3).

In all samples, both amplitude hysteresis due to internal friction (IT) and the Young's modulus (YM) are present, in other words, the dependences measured sequentially during increasing or decreasing amplitudes do not coincide with each other. The dependence measured during a decreasing amplitude is located above the dependence measured with an increasing amplitude. This behavior is characteristic of various types of single crystals and polycrystals [30, 31]. From the theoretical perspective, the amplitude hysteresis indicates the oscillatory motion of dislocations in the force fields of stops that secure dislocations of point defects [32, 33]. The hysteresis depends on the maximum strain amplitude at which the dependences were taken. For example, hysteresis was not observed at an amplitude of less than 10^{-5} (blue curves). A further slight increase

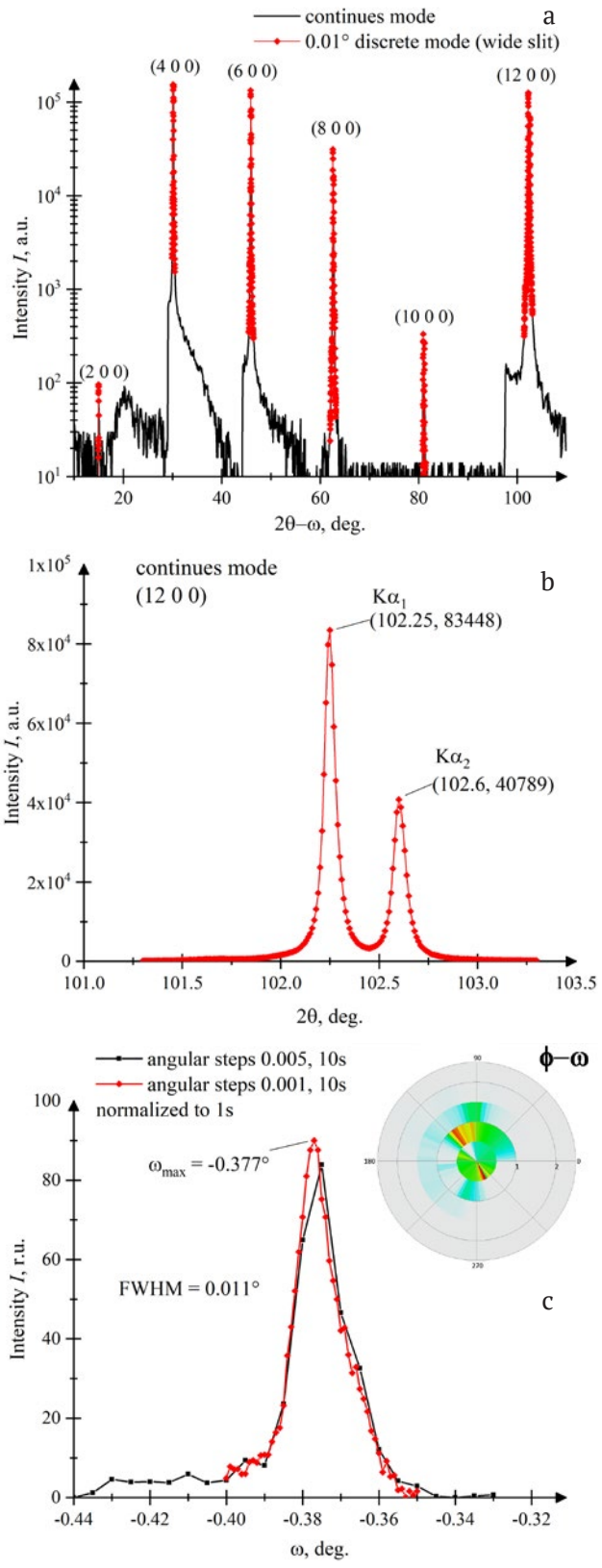

Fig. 2. The X-ray diffraction of the central region of the β-Ga_2O_3 sample over a wide range of angles (a), profile and rocking curve of the maximum (12 0 0) (b) and (c) respectively

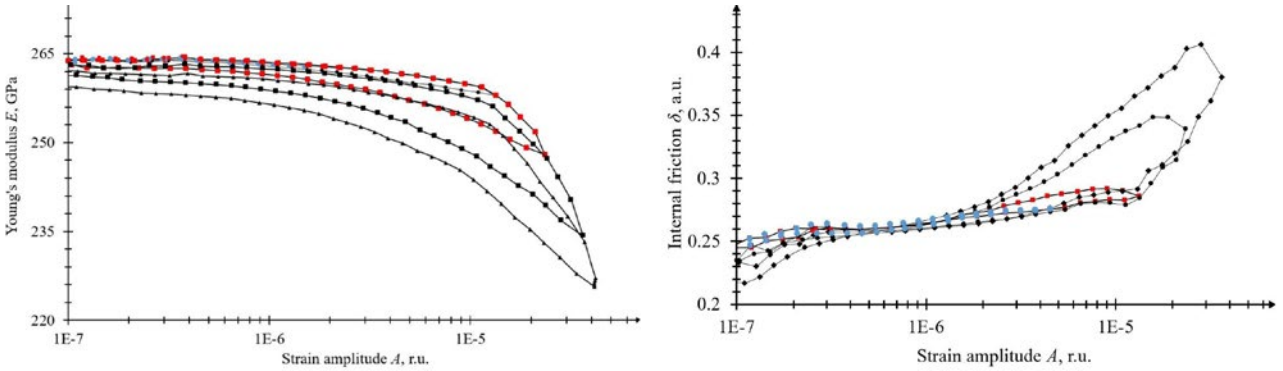

a b

Fig. 3. Dependences of Young's modulus (a) and internal friction (b) on strain amplitude at room temperature

in amplitude (red curves) resulted in the appearance of a small reversible hysteresis. At amplitudes considerably higher than 10^{-5} (black curves), there were large reversible and irreversible hystereses.

These curves can be divided into two stages: (i) low-amplitude, characterized by a moderate increase in IF and a fall in the YM; (ii) high-amplitude with a significant increase in IF and a fall in the YM. During the first stage, there were vibrations of dislocations trapped at point defects (pinning centers) in the form of impurity atoms and vacancies and during the second stage, vibrations of dislocations appeared after the detachment [30]. The transition from the first stage to the second occurred at a strain amplitude of about 10^{-5}.

Fig. 4 shows the Young's modulus defect caused by the deformation of Ga_2O_3 samples. The curves were taken at three temperatures: 300, 225, and 118 K. In this case, the amplitude dependences of the Young's modulus defect are associated with the two stages of the sample microdeformation described above. Despite the fact that the YM defect is determined primarily by the density of defect structures and their distribution over the section and length of the studied sample, the temperature also has a significant impact on this characteristic [30]. When the temperature rose, the growth of the YM defect was due to unlocking dislocations [34]. It should be noted that the graph was built from the dependences $E(\varepsilon)$ taken at the very

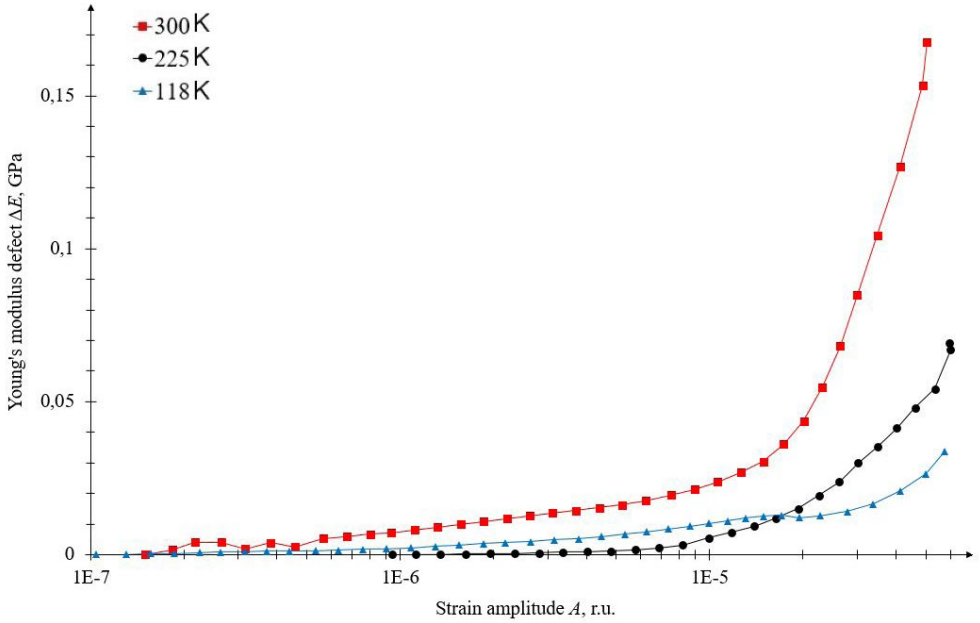

Fig. 4. Amplitude dependence of the Young's modulus defect

first increase in amplitude on samples that had never been exposed to high amplitudes.

Fig. 5 shows the temperature dependences of the YM and IF. On the whole, when the temperature decreased, the Young's modulus increased, while the IF decreased. This behavior of dependences of mechanical characteristics is conventional. There was also a slight gap in the dependences around 273 K, apparently due to the presence of residual moisture in the measuring cell. It should be noted that the YM was in the range of 261–272 GPa (Fig. 5a) and at room temperature it fully correlated with the data presented in other papers [35, 36]. For example, the authors of [35] studied nanomechanical resonators based on β-Ga_2O_3 nano flakes grown by low pressure chemical vapor deposition (LPCVD). The measurements taken in this paper revealed the Young's modulus E = 261 GPa and anisotropic biaxial inline tension of 37.5 and 107.5 MPa. At a temperature of about 280 K, there was an IF peak (Fig. 5b), while on the YM temperature dependence there was an inflection. This peak and inflection are associated with dislocation interactions, apparently with Hasiguti relaxation or Snoek–Koster relaxation [37]. Hasiguti relaxation is associated with the interaction of dislocations (inflections) with their intrinsic defects: interstitial defects, vacancies, and their complexes. In our case, Snoek–Koster relaxation can be due to the "dragging" or "separation" of impurity atmospheres during the motion of dislocations. The obtained results can be associated with the technology of obtaining monocrystalline intergrowths. At growth temperatures, the melt is unstable and subject to decomposition into gas components: divalent gallium oxide, monovalent oxide, metallic gallium, and oxygen: (Ga_2O_3 → GaO → Ga_2O → Ga, and O). This process cannot be fully compensated for by an excess of oxygen in the growth atmosphere, which, as a rule, leads to the emergence of oxygen vacancies in the growing bulk crystal [38]. Hence, it can be assumed that the Hasiguti relaxation is the main mechanism responsible for the formation of the IF peak and the inflection on the YM dependence. However, further research is required to reliably prove the determined nature of the peaks. When comparing equivalent samples of the same initial material, the Hasiguti relaxation peaks in some of them can be annealed during the reverse stage [37].

3. Conclusion

The obtained diffraction curve profile (Fig. 2a) and the value of the parameter a of the crystal lattice of the synthesized monoclinic phase correspond to the reference data in the PDF database and the data presented in other scientific publications [39], which may indicate a high degree of structural perfection of the obtained β-Ga_2O_3 samples and a small value of residual stresses in the crystal. The small value (for the used slit configuration) of the half-width of the rocking curve indicates a high degree of crystalline perfection of the studied region within the sample. An inconsiderable asymmetry of this curve in the

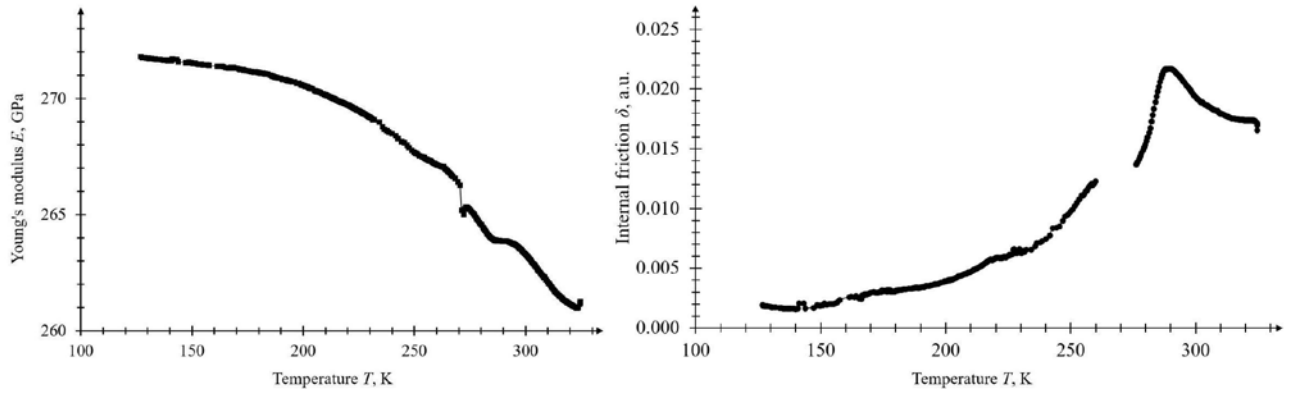

a b

Fig. 5. Temperature dependences of Young's modulus (a) and internal friction (b) of Ga_2O_3

area of small angles can be due to various factors, such as the small-angle disorientation of blocks (grains) or the presence of twins. The crystal structure of the studied samples corresponds to the initial material [11, 12].

The PCO technique was used to obtain the mechanical characteristics of the samples at a frequency of 100 kHz. During the experiments, the amplitude dependences of the YM and IF were obtained and interpreted. The amplitude dependences can be divided into two stages: (i) low-amplitude, in which vibrations of dislocations occur within impurity atmospheres; (ii) high-amplitude, in which vibrations of dislocations occur outside impurity atmospheres. The value of strain amplitude was found at which there is the transition from the first stage to the second. As a result, the temperature dependences of the YM and IF at a frequency of about 100 kHz were obtained for β-Ga_2O_3. Those dependences are in line with the results of other experiments. Further research is required to interpret the nature of the IF relaxation peak at 285 K associated with dislocation interactions.

Contribution of the authors

The authors contributed equally to this article.

Conflict of interests

The authors declare that they have no known competing financial interests or personal relationships that could have influenced the work reported in this paper.

References

1. Kitsay A. A., Nosov YU. G., CHikiryaka A. V., Nikolaev V. I. Growth of β-Ga_2O_3 single crystals by the solution-melt method. *Technical Physics Letters*. 2023;49(14): 16–18. https://doi.org/10.21883/PJTF.2023.14.55819.19589

2. Kalygina V. M., Nikolaev V. I., Almaev A. V., Tsymbalov A. V., Petrova Y. S., Pechnikov I. A., Butenko P. N. Properties of resistive structures based on gallium oxide polymorphic phases. *Technical Physics Letters*. 2020;46: 867–870. https://doi.org/10.1134/S1063785020090060

3. Green A. J., Speck J., Xing G., ... Higashiwaki M. β-gallium oxide power electronics. *Apl Materials*. 2022;10(2): 029201. https://doi.org/10.1063/5.0060327

4. Kalygina V. M., Lygdenova T. Z., Petrova Y. S., Chernikov E. V. Influence of the substrate material on the properties of gallium-oxide films and gallium-oxide-based structures. *Semiconductors*. 2019;53(4): 452–457. https://doi.org/10.1134/S1063782619040122

5. Kaur D., Kumar M. A strategic review on gallium oxide based deep-ultraviolet photodetectors: recent progress and future prospects. *Advanced Optical Materials*. 2021;9(9): 2002160. https://doi.org/10.1002/adom.202002160

6. Kalygina V. M., Kiselyeva O. S., Kushnarev B. O., Oleinik V. L., Petrova Y. S., Tsymbalov A. V. Self-powered photo diodes based on Ga_2O_3/n-GaAs structures. *Semiconductors*. 2022;56(9): 707–711. https://doi.org/10.21883/SC.2022.09.54139.9868

7. Lu X., Zhou L., Chen L., Ouyang X., Liu B., Xu J., Tang H. Schottky X-ray detectors based on a bulk β-Ga_2O_3 substrate. *Applied Physics Letters*. 2018;112(10): 103502 https://doi.org/10.1063/1.5020178

8. Zhu J., Xu Z., Ha S., Li D., Zhang K., Zhang H., Feng J. Gallium oxide for gas sensor applications: A comprehensive review. *Materials*. 2022:15(20): 7339. https://doi.org/10.3390/ma15207339

9. Nikolaev V. I., Almaev A. V., Kushnarev B. O., ... Chernikov E. V. Gas-sensing properties of In_2O_3-Ga_2O_3 alloy films. *Technical Physics Letters*. 2022;48(7): 76–79. https://doi.org/10.21883/TPL.2022.07.54046.19211

10. Petrenko A. A., Kovach Ya. N., Bauman D. A., Odnoblyudov M. A., Bougrov V. E., Romanov A. E. Current state of Ga_2O_3-based electronic and optoelectronic devices. Brief review. *Reviews on Advanced Materials and Technologies*. 2021;3(2): 1–26. https://doi.org/10.17586/2687-0568-2021-3-2-1-26

11. Bauman D. A., Panov D. Iu., Spiridonov V. A... Romanov A. E. High quality β-Ga_2O_3 bulk crystals, grown by edge-defined film-fed growth method: growth features, structural and thermal properties. *Journal of Vacuum Science and Technology A*. 2023;41: 053203. https://doi.org/10.1116/6.0002644

12. Bauman D. A., Panov D. I., Spiridonov V. A., Kremleva A. V., Romanov A. E. On the successful growth of bulk gallium oxide crystals by the EFG (Stepanov) method. *Functional Materials Letters*. 2023: 2340026. https://doi.org/10.1142/S179360472340026X

13. Son N. T., Goto K., Nomura K., ... Janzén E. Electronic properties of the residual donor in unintentionally doped β-Ga_2O_3. *Journal of Applied Physics*. 2016;120(23): 235703. https://doi.org/10.1063/1.4972040

14. Ivanova E. V., Dementev P. A., Zamoryanskaya M. V., ... Bougrov V. E. Study of charge carrier traps in bulk crystal gallium oxide β-Ga_2O_3. *Physics of the Solid State*. 2021;63(4): 544–549. https://doi.org/10.1134/S1063783421040089

15. Wang Z., Chen X., Ren F. F., Gu S., Ye J. Deep-level defects in gallium oxide. *Journal of Physics D: Applied Physics*. 2020;54(4): 043002. https://doi.org/10.1088/1361-6463/abbeb1

16. Manikanthababu N., Sheoran H., Siddham P., Singh R. Review of radiation-induced effects on

β-Ga_2O_3 materials and devices. *Crystals*. 2022;12(7): 1009. https://doi.org/10.3390/cryst12071009

17. Seyidov P., Ramsteiner M., Galazka Z., Irmscher K. Resonant electronic Raman scattering from Ir^{4+} ions in β-Ga_2O_3. *Journal of Applied Physics*. 2022;131(3): 035707. https://doi.org/10.1063/5.0080248

18. Abdrakhmanov V. L., Zav'yalov D. V., Konchenkov V. I., Kryuchkov S. V. Effect of a strong electromagnetic wave on the conductivity of β-Ga_2O_3. *Bulletin of the Russian Academy of Sciences: Physics*. 2020;84(1): 53-57. https://doi.org/10.3103/S1062873820010037

19. Guzilova L. I., Grashchenko A. S., Pechnikov A. I., ... Nikolaev V. I. *Materials Physics and Mechanics*. 2016;29(2): 166–171. (In Russ., abstract in Eng.). Available at: https://www.ipme.ru/e-journals/MPM/no_22916/MPM229_09_guzilova.pdf

20. Quimby S. L. On the experimental determination of the viscosity of vibrating solids. *Physical Review*. 1925;25(4): 558. https://doi.org/10.1103/PhysRev.25.558

21. Kimball A. L., Lovell D. E. Internal friction in solids. *Physical Review*. 1927;30(6): 948. https://doi.org/10.1103/PhysRev.30.948

22. Marx J. Use of the piezoelectric gauge for internal friction measurements. *Review of Scientific Instruments*. 1951;22(7): 503–509. https://doi.org/10.1063/1.1745981

23. Naimi E. K. Internal-friction anisotropy in a real crystal and construction of characteristic internal-friction surfaces. *Soviet Physics Journal*. 1975;18: 371–375. https://doi.org/10.1007/BF00889303

24. Granato A. V., Lücke K. Application of dislocation theory to internal friction phenomena at high frequencies. *Journal of Applied Physics*. 1956;27(7): 789–805. https://doi.org/10.1063/1.1722485

25. Robinson W. H., Edgar A. The piezoelectric method of determining mechanical damping at frequencies of 30 to 200 KHz. *IEEE Transactions on Sonics and Ultrasonics*. 1974;21(2): 98–105. https://doi.org/10.1109/T-SU.1974.29798

26. Tyapunina N. A., Zinenkova G. M., Shtrom E. V. Dislocation multiplication in alkali halide crystals exposed to ultrasonic waves. The original stage. *Physica Status Solidi (a)*. 1978;46(1): 327–336. https://doi.org/10.1002/pssa.2210460143

27. Nikolaev V. I., Stepanov S. I., Romanov A. E., Bougrov V. E. Gallium oxide. In: *Single Crystals of Electronic Materials*. R. Fornari (ed.). Woodhead Publishing; 2019. 487–521. https://doi.org/10.1016/B978-0-08-102096-8.00014-8

28. Yamaguchi H., Kuramata A., Masui T. Slip system analysis and X-ray topographic study on β-Ga_2O_3. *Superlattices and Microstructures*. 2016;99: 99–103. https://doi.org/10.1016/j.spmi.2016.04.030

29. Wu Y., Rao Q., Best J. P., Mu D., Xu X., Huang H. Superior room temperature compressive plasticity of submicron beta-phase gallium oxide single crystals. *Advanced Functional Materials*. 2022;32(48): 2207960. https://doi.org/10.1002/adfm.202207960

30. Kaminskii V. V., Kalganov D. A., Podlesnov E., Romanov A. E. Influence of dislocation and twin structures on the mechanical characteristics of Ni-Mn-Ga alloys at ultrasonic frequencies. *Frontier Materials and Technologies*. 2022;2: 28–36. https://doi.org/10.18323/2782-4039-2022-2-28-36

31. Kaminskii V. V., Lyubimova Y. V., Romanov A. E. Probing of polycrystalline magnesium at ultrasonic frequencies by mechanical spectroscopy. *Materials Physics and Mechanicals*. 2020;44(1): 19–25. https://doi.org/10.18720/MPM.4412020_3

32. Guzilova L. I., Kardashev B. K., Pechnikov A. I., Nikolaev V. I. Elasticity and Inelasticity of bulk GaN crystals. *Technical Physics*. 2020;90(1): 138–142. https://doi.org/10.1134/s1063784220010089

33. Sapozhnikov K. V., Golyandin S. N., Kustov S. B. Amplitude dependence of the internal friction and young's modulus defect of polycrystalline indium. *Physics of the Solid State*. 2010;52(1): 43–48. https://doi.org/10.1134/S1063783410010087

34. Lebedev A. B., Kustov S. V., Kardashov B. K. On internal friction and the Young's modulus defect in the crystal deformation process*. *Solid State Physics*. 1992;34(9): 2915. (In Russ.). Available at: https://journals.ioffe.ru/articles/viewPDF/22631

35. Zheng X. Q., Lee J., Rafique S., Han L., Zorman C. A. Zhao H., Feng P. X. L. Ultrawide band gap β-Ga_2O_3 nanomechanical resonators with spatially visualized multimode motion. *ACS Applied Materials and Interfaces* 2017;9(49): 43090–43097. https://doi.org/10.1021/acsami.7b13930

36. Zheng X. Q., Zhao H., Feng P. X. L. A perspective on β-Ga_2O_3 micro/nanoelectromechanical systems. *Applied Physics Letters*. 2022;120(4). https://doi.org/10.1063/5.0073005

37. Golovin I. S. Internal friction and mechanical spectroscopy of metals and alloys. *Metal Science and Heat Treatment*. 2012;54(5-6): 207–208. https://doi.org/10.1007/s11041-012-9482-7

38. Zakgeim D. A., Panov D. I., Spiridonov V. A., ... Bougrov V. E. Volume gallium oxide crystals grown from melt by the Czochralski method in an oxygen-containing atmosphere. *Technical Physics Letters*. 2020;46: 1144–1146. https://doi.org/10.1134/S1063785020110292

39. Samoylov A. M., Kopytin S. S., Oreshkin K. V., Shevchenko E. A. Synthesis of chemically pure β-phase powders of gallium(III) oxide. *Condensed Matter and Interphases*. 2022;24(3): 345–355. https://doi.org/10.17308/kcmf.2022.24/9857

**Translated by author of the article.*

Information about the authors

Vladimir V. Kaminskii, Cand. Sci. (Phys.–Math.), Head of the Laboratory, ITMO University (Saint Petersburg, Russian Federation).
https://orcid.org/0000-0002-4388-2459
vvkaminskii@itmo.ru

Dmitrii A. Kalganov, Junior Researcher at the Advanced Data Transfer System Institute, ITMO University (Saint Petersburg, Russian Federation).
https://orcid.org/0000-0003-1986-3693
kalganov@itmo.ru

Dmitrii I. Panov, Cand. Sci. (Phys.–Math.), Head of the Laboratory, ITMO University (Saint Petersburg, Russian Federation).
https://orcid.org/0000-0001-8715-9505
dmitriipnv@itmo.ru

Vladislav A. Spiridonov, Engineer at the Advanced Data Transfer System Institute, ITMO University (Saint Petersburg, Russian Federation).
https://orcid.org/0000-0001-5751-8597
vladspiridonov@itmo.ru

Andrey I. Ivanov, Engineer at the Advanced Data Transfer System Institute, ITMO University (Saint Petersburg, Russian Federation).
https://orcid.org/0000-0003-0737-9079
aiivanov@itmo.ru

Margarita V. Rozaeva, master student, Engineer at the Advanced Data Transfer System Institute, ITMO University (Saint Petersburg, Russian Federation).
https://orcid.org/0009-0000-2978-5380
412189@niuitmo.ru

Dmitrii A. Bauman, Cand. Sci. (Phys.–Math.), Associate Professor at the Advanced Data Transfer System Institute, ITMO University (Saint Petersburg, Russian Federation).
https://orcid.org/0000-0002-5762-5920
dabauman@itmo.ru

Alexey E. Romanov, Dr. Sci. (Chem.), Professor, Head of the Advanced Data Transfer System Institute, ITMO University (Saint Petersburg, Russian Federation).
https://orcid.org/0000-0003-3738-408X
aeromanov@itmo.ru

Received 20.09.2023; approved after reviewing 13.10.2023; accepted for publication 16.10.2023; published online 26.12.2023.

Translated by Irina Charychanskaya